

Amplification of fluctuations in a spinor Bose-Einstein condensate

S. R. Leslie,^{1,*} J. Guzman,^{1,2} M. Vengalattore,¹ Jay D. Sau,¹ Marvin L. Cohen,^{1,2} and D. M. Stamper-Kurn^{1,2}

¹*Department of Physics, University of California-Berkeley, Berkeley, California 94720, USA*

²*Materials Sciences Division, Lawrence Berkeley National Laboratory, Berkeley, California 94720, USA*

(Received 9 June 2008; revised manuscript received 8 August 2008; published 28 April 2009)

Dynamical instabilities in a ^{87}Rb $F=1$ spinor Bose-Einstein condensate are used as a parametric amplifier of quantum spin fluctuations. We demonstrate the spectrum of this amplifier to be tunable, in quantitative agreement with theory. We quantify the microscopic spin fluctuations of the initially paramagnetic condensate by applying this amplifier and measuring the resulting macroscopic magnetization. The variance of these fluctuations agrees with predictions of a beyond-mean-field theory. This spin amplifier is thus shown to be nearly quantum limited at a gain as high as 30 dB.

DOI: [10.1103/PhysRevA.79.043631](https://doi.org/10.1103/PhysRevA.79.043631)

PACS number(s): 03.75.Mn, 05.30.Jp, 42.50.-p, 75.45.+j

Accompanied by a precise theoretical framework and prepared in a highly controlled manner, ultracold atomic systems serve as a platform for studies of quantum dynamics and many-body quantum phases, and as a potential resource for precise sensors. Among these systems, gaseous spinor Bose-Einstein condensates [1–5], in which atoms may explore all sublevels of the hyperfine spin F , give access to interesting static and dynamical properties of a magnetic superfluid [6–9] and can serve as a medium for precise magnetometry [10].

Particularly interesting dynamics is associated with a quantum phase transition between a paramagnetic and a ferromagnetic phase in an $F=1$ spinor Bose-Einstein condensate [8]. This transition is crossed as the quadratic Zeeman energy term, of the form qF_z^2 , is tuned through a critical value $q=q_0$. Here, F_z is the longitudinal (\hat{z} axis) projection of the dimensionless vector spin \mathbf{F} . This phase transition is accompanied by the onset of dynamical instabilities in a condensate prepared in the paramagnetic state, with macroscopic occupation of the $|m_z=0\rangle$ state [11–13]. The instabilities cause transverse spin perturbations to grow, producing atoms into the $|m_z=\pm 1\rangle$ sublevels. In contradiction with the mean-field prediction that the paramagnetic state should remain stationary because it lacks fluctuations by which to seed the instability, experiments revealed the spontaneous magnetization of such condensates after they were quenched across the phase transition by a rapid change in q .

Here, we consider making use of dynamical instabilities in a quenched spinor condensate to realize a mode-by-mode low-noise parametric amplifier of magnetization. Low-noise amplifiers have been developed in myriad physical systems to enable precision measurements and studies of quantum noise. For example, parametric amplifiers constructed with Josephson junctions have been used to measure weak microwave signals and to induce squeezing of microwave fields [14]. Similarly, quantum-limited amplification of spin excitations in spinor condensates could lead to the preparation of spin-squeezed states, with applications toward metrology.

In this paper, following studies of solid-state low-noise amplifiers ([14,15], for example), we characterize the spin-

mixing amplifier by seeding it with broadband noise and measuring precisely the spectrum of its output. We present two main results. First, we characterize the spectrum of the spin-mixing amplifier and demonstrate it to be tunable by varying the quadratic Zeeman shift. This spectrum compares well with a theoretical model that accounts for the inhomogeneous condensate density and for magnetic dipole interactions. Second, we measure precisely the transverse magnetization produced by this amplifier at various stages of amplification, up to a gain of 30 dB in the magnetization variance. Under the assumption that the system performs as a quantum-limited amplifier with the aforementioned spectral gain profile, this magnetization signal corresponds to the amplification of initial fluctuations with a variance slightly greater than that expected for zero-point fluctuations of the quantized spin-excitation modes that become unstable.

Descriptions of the dynamics of initially paramagnetic spinor condensates [12,13,16–19] have focused on the effects of the quadratic Zeeman energy and of the spin-dependent contact interaction. The latter has the mean-field energy density $c_2 n \langle \mathbf{F} \rangle^2$ and, with $c_2 = 4\pi\hbar^2 \Delta a / 3m < 0$, favors a ferromagnetic state. Here, $\Delta a = (a_2 - a_0)$, where $a_{F_{\text{tot}}}$ is the s -wave scattering length for collisions between particles of total spin F_{tot} , and m is the atomic mass. Excitations of the uniform condensate include both the scalar density excitations and also two polarizations of spin excitations with a dispersion relation given as $E_s^2(\mathbf{k}) = (\varepsilon_k + q)(\varepsilon_k + q - q_0)$, where $\varepsilon_k = \hbar^2 k^2 / 2m$ and $q_0 = 2|c_2|n$. For $q > q_0$, spin excitations are gapped ($E_s^2 > 0$), and the paramagnetic condensate is stable. Below this critical value, the paramagnetic phase develops dynamical instabilities, defined by the condition $E_s^2 < 0$, that amplify transverse magnetization. The dispersion relation defines the spectrum of this amplification, yielding a wave-vector-dependent time constant for exponential growth of the power in the unstable modes, $\tau = \hbar / 2\sqrt{|E_s^2|}$.

The unstable regime is divided further into two regions. Near the critical point, reached by a “shallow” quench to $q_0/2 \leq q < q_0$, the fastest-growing instability occurs at zero wave vector, favoring the “light-cone” evolution of magnetization correlations at ever longer range [12]. For a “deep” quench, with $q < q_0/2$, the instabilities reach a maximum growth rate of $1/\tau = q_0/\hbar$. The nonzero wave vector of this dominant instability sets the size of magnetization domains produced following the quench.

*sleslie@berkeley.edu

Similarly as in previous work [8], we produce condensates of $N_0=2.0 \times 10^6$ ^{87}Rb atoms, with a peak density of $n=2.6(1) \times 10^{14} \text{ cm}^{-3}$ and a kinetic temperature of $\approx 50 \text{ nK}$, trapped in a linearly polarized optical dipole trap characterized by trap frequencies $(\omega_x, \omega_y, \omega_z)=2\pi \times (39, 440, 4.2) \text{ s}^{-1}$. Taking $\Delta a = -1.4(3) a_B$ [20], with a_B being the Bohr radius, the spin healing length $\xi_s = (8\pi m |\Delta a|)^{-1/2} = 2.5 \text{ } \mu\text{m}$ is larger than the condensate radius $r_y = 1.6 \text{ } \mu\text{m}$ along the imaging axis (\hat{y}). Thus, the condensate is effectively two dimensional with respect to spin dynamics. For this sample, $q_0 = 2|c_2 \langle n \rangle = h \times 15 \text{ Hz}$ given the maximum \hat{y} -averaged condensate density $\langle n \rangle$.

The quadratic Zeeman shift arises from the application of both static and modulated magnetic fields. A constant field of magnitude B , directed along the long axis of the condensate, leads to a quadratic shift of $q_B/h = (70 \text{ Hz/G}^2) B^2$. In addition, a linearly polarized microwave field [21], with Rabi frequency Ω and detuned by $\delta/2\pi = \pm 35 \text{ kHz}$ from the $|F=1, m_z=0\rangle$ to $|F=2, m_z=0\rangle$ hyperfine transition, induces a quadratic (ac) Zeeman shift of $q_\mu = -\hbar \Omega^2 / 4\delta$ [22].

The condensate is prepared in the $|m_z=0\rangle$ state using rf pulses followed by application of a 6 G/cm magnetic field gradient that expels atoms in the $|m_z = \pm 1\rangle$ states from the trap [8]. This preparation takes place in a static 4 G field and with no microwave irradiation, setting $q = q_B + q_\mu > q_0$ so that the paramagnetic condensate is stable. Next, we increase the microwave field strength to a constant value, corresponding to a Rabi frequency in the range of $2\pi \times (0-1.5) \text{ kHz}$, to set q_μ . To switch on the amplifier, we ramp the magnetic field over 5 ms to a value of $B=230 \text{ mG}$ (giving $q_B/h=7.6 \text{ Hz}$). During separate repetitions of the experiment (for different values of q_μ), the quadratic Zeeman shift at the end of the ramp was thus brought to final q_f/h values between -2 and 16 Hz .

Following the quench, the condensate spontaneously develops macroscopic transverse magnetization, saturating within about 110 ms to a pattern of spin domains, textures, vortices, and domain walls [8]. Using a 2-ms-long sequence of phase-contrast images, we obtain a detailed map of the column-integrated magnetization $\tilde{\mathbf{M}}$ at a given time after the quench [10]. The experiment is then repeated with a new sample.

The observed transverse magnetization profiles [23] of spinor condensates (Fig. 1) confirm the salient features predicted for the spin-mixing amplifier. The variation in the amplifier's spatial spectrum with q_f is reflected in the characteristic size of the spin domains, taken as the minimum distance from the origin at which the magnetization correlation function,

$$G(\delta\mathbf{r}) = \frac{\sum_{\mathbf{r}} \tilde{\mathbf{M}}(\mathbf{r} + \delta\mathbf{r}) \cdot \tilde{\mathbf{M}}(\mathbf{r})}{(g_F \mu_B)^2 \sum_{\mathbf{r}} \tilde{n}(\mathbf{r} + \delta\mathbf{r}) \tilde{n}(\mathbf{r})}, \quad (1)$$

acquires its first minimum. Here $g_F \mu_B$ is the atomic magnetic moment and \tilde{n} is the \hat{y} -integrated column density. This characteristic size increases with increasing q_f (Fig. 2). For $q_f/h \geq 9 \text{ Hz}$, the magnetization features become long

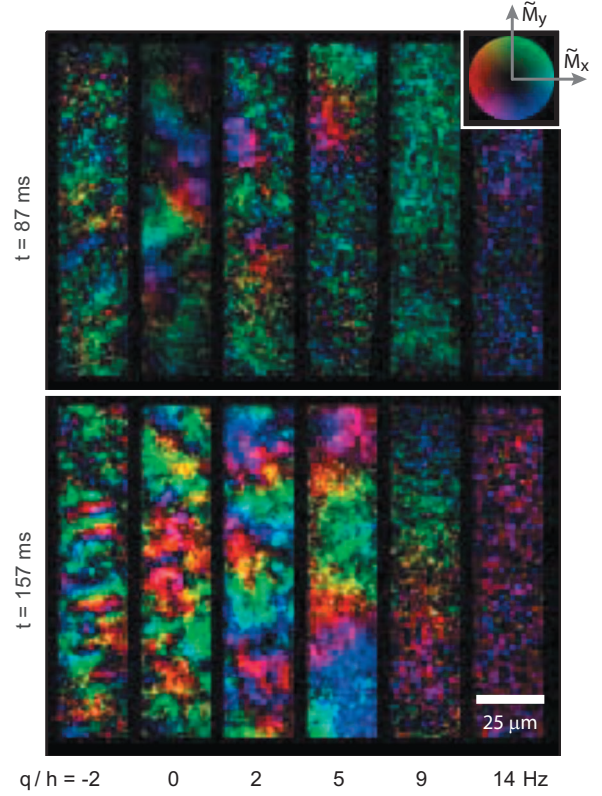


FIG. 1. (Color) Transverse magnetization produced near the condensate center after 87 ms (top) and 157 ms (bottom) of amplification at variable q_f . Magnetization orientation is indicated by hue and amplitude is indicated by brightness (color wheel shown). The characteristic spin-domain size grows as q_f increases. The reduced signal strength for $q_f/h \geq 9 \text{ Hz}$ reveals the diminished gain of the spin-mixing amplifier.

ranged, as predicted. An exact determination of their characteristic size then becomes limited by residual magnetic field inhomogeneities ($< 2 \text{ } \mu\text{G}$).

The data also confirm the distinction between deep and shallow quenches. The spatially averaged magnetization

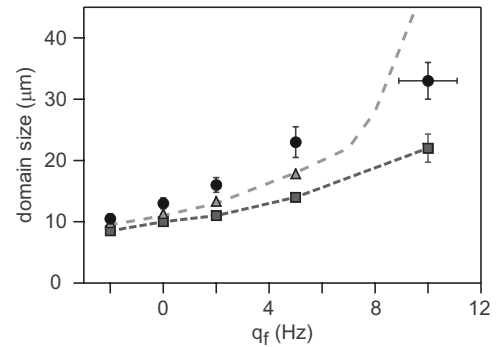


FIG. 2. Characteristic domain size after 87 ms of amplification at variable q_f . Data (circles) are averages over five experimental repetitions; error bars are statistical. Horizontal error bar reflects systematic uncertainty in q_f . Predictions based on numerical simulations for $|\Delta a| = 1.45 a_B$ [7] (squares) and $1.07 a_B$ [24] (triangles) are shown, with error bar reflecting systematic uncertainty in the atomic density.

strength during the amplification, quantified by $G(0)$ at $t = 87$ ms after the quench, is found to be constant for $0 < q_f/h < 6$ Hz, reflecting the gain of the amplifier being uniform over $0 \leq q \leq q_0/2$ [12]. For shallow quenches, with $q_f/h \geq 7$ Hz, the measured magnetization decreases, reflecting a diminishing gain as q_f increases up to the transition point.

While the above observations agree with theoretical predictions, we note the unexpected and unexplained outcome of quenches to negative values of q_f . That is, for quenches to $q_f/h \leq -7$ Hz, obtained using stronger microwave-driven shifts than described above, the growth of magnetization was greatly suppressed [$G(0)|_{t=160 \text{ ms}} \leq 10^{-2}$].

Having characterized the spin-mixing amplifier, let us consider the source of its input signal. For this, we develop a quantum field description of the spin-mixing instability [12,19], working in the polar spin basis, where $\hat{\phi}_{n,k}$ is the annihilation operator for atoms of wave vector k in the zero-eigenvalue states of $\mathbf{F} \cdot \mathbf{n}$. Treating a uniform condensate within the Bogoliubov approximation, one defines mode operators $\hat{b}_{n,k} = u\hat{\phi}_{n,k} + v\hat{\phi}_{n,-k}^\dagger$ for the two polarizations of transverse [$n \in \{x, y\}$] spin excitations. The portion of the spin-dependent Hamiltonian representing dynamic instabilities, H_{DI} , is then approximated as representing a set of parametric amplifiers:

$$H_{\text{DI}} = -\frac{i}{2} \sum_k |E_s(k)| (b_{x,k}^2 - b_{x,k}^{\dagger 2} + b_{y,k}^2 - b_{y,k}^{\dagger 2}). \quad (2)$$

The parametric amplifiers serve to squeeze the initial state in each spin-excitation mode, amplifying one quadrature of $b_{n,k}$ and deamplifying the other.

The above treatment may be recast in terms of spin fluctuations atop the paramagnetic state: fluctuations in the transverse spin, represented by the observables F_x and F_y , and fluctuations in the alignment of the spinor, represented by the components N_{yz} and N_{xz} of the spin quadrupole tensor. We identify the Bogoliubov operators defined above as linear combinations of these observables. Based on this identification, we draw two conclusions. First, an ideally prepared paramagnetic condensate is characterized by quantum fluctuations in the Bogoliubov modes. In the linear regime, fluctuations in $b_{x,k}$ ($b_{y,k}$) correspond to projection noise for the conjugate observables F_x (F_y) and N_{yz} (N_{xz}). Second, the dynamical instabilities lead to a coherent amplification of these initial shot-noise fluctuations. While in the present work we observe only the magnetization, in future work both quadratures of the spin-mixing amplifier may be measured using optical probes [25] or by using quadratic Zeeman shifts to rotate the spin quadrature axes.

To test the validity of this description, we evaluate $G(0)|_t$, the magnetization variance after an interval t of amplification, over the central region of the condensate. As shown in Fig. 3, $G(0)|_t$ rises above our detection noise floor for $t \gtrsim 40$ ms. We consider the linear-amplification theory to be applicable for $t \leq 90$ ms, and, following Ref. [12], perform a least-squares fit to a function of the form

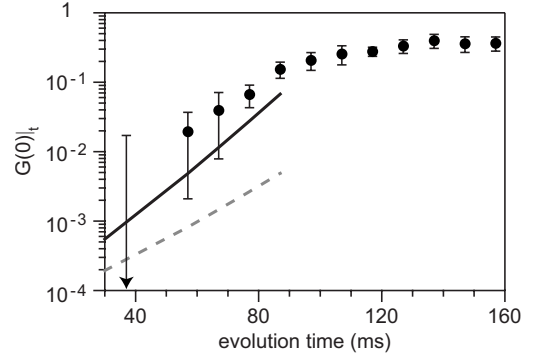


FIG. 3. Temporal evolution of the transverse magnetization variance $G(0)|_t$ at $q_f = 2$ Hz, evaluated over the central $16 \times 124 \mu\text{m}^2$ region of the condensate and averaging over eight experimental repetitions; error bars are statistical. The contribution to $G(0)|_t$ from imaging noise was subtracted from the data. Predictions from numerical calculations for $|\Delta a| = 1.45 a_B$ and $1.07 a_B$ are shown as black and grey lines, respectively.

$$G(0)|_t = G(0)|_{t_m} \times \sqrt{t/t_m} e^{(t-t_m)/\tau}. \quad (3)$$

Here τ is the time constant characterizing the growth rate of the magnetization variance and $t_m = 77$ ms.

To compare our measurements to the amplifier theory outlined above, we performed numerical calculations of $G(0)|_t$, taking into account the inhomogeneous density profile, dipolar interactions, and quantum fluctuations of the initial state [26]. We simulate the condensate dynamics using the truncated Wigner approximation (TWA); i.e., we evolve classical spin fluctuations, whose initial variance is quantum limited in magnitude, according to the Gross-Pitaevskii equation. This treatment is exact in the linear-amplification regime, and also provides an approximate description of nonlinear behavior associated with depletion of the $|m=0\rangle$ population and with intermode coupling. To solve the Gross-Pitaevskii equation numerically, we employ a sixth-order Runge-Kutta method with time and position-space resolutions of $3.5 \mu\text{s}$ and $0.5 \mu\text{m}$, respectively. In contrast to the linear homogeneous case, which has been previously studied using momentum-space spin-excitation modes [12,13], the nonlinear inhomogeneous case requires the use of proper position-space modes. Our calculations show the rate of growth of magnetization fluctuations to be smaller than that indicated by the maximum condensate density, owing to the inhomogeneous density profile of the trapped gas. The asymmetric trap potential also causes the calculated magnetization correlations to be stronger along the long axis of the trapping potential [27], a tendency that is supported by our observations (Fig. 1). For our experimental settings, the calculation indicates that dipolar interactions serve to increase slightly the time constant and decrease the length scale which characterize the formation of transversely magnetized domains in the condensate.

From such simulations, we determined theoretical values of $G(0)|_t$ for several values of the scattering length difference Δa within the range of recent measurements [7,24]. As shown in Figs. 3 and 4, our data are consistent with the

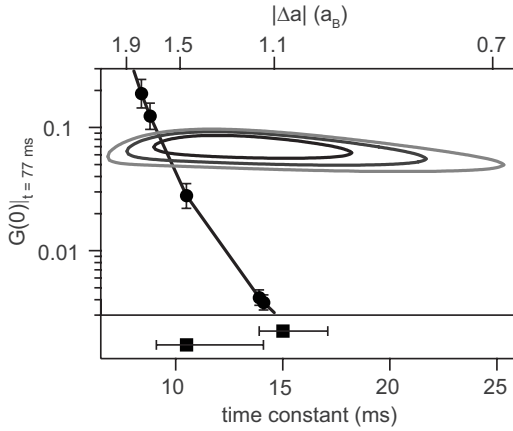


FIG. 4. The magnetization variance $G(0)|_{t=77 \text{ ms}}$ at $t_m=77 \text{ ms}$ and exponential time constant τ of the amplifier, obtained by fitting data in Fig. 3 corresponding to $57 \leq t \leq 87 \text{ ms}$, are indicated by contours of the 1, 2, and 3 σ confidence regions using a χ^2 test. Predictions from numerical calculations of the quantum amplification theory, assuming different values of $|\Delta a|$, are shown (circles and interpolating line). Error bars reflect systematic uncertainties in the condensate density, by which the time constant is related to the value of Δa , and in q_f . Time constants corresponding to reported values for $|\Delta a|$ are indicated at bottom.

quantum-limited amplification of zero-point quantum fluctuations in the case that $|\Delta a|$ lies in the upper range of its reported values. Alternatively, under the assumption that the observed amplification of spin fluctuations is quantum limited, taking the best-fit value of $\tau=12 \text{ ms}$, the variance of initial spin fluctuations in our paramagnetic sample is measured to be roughly five times larger than that of purely quantum fluctuations.

We performed several investigations to identify possible technical or thermal contributions to the spin fluctuations of our samples. A bound on such noise was obtained by performing a Stern-Gerlach analysis of populations N_{\pm} in the $|m_z = \pm 1\rangle$ states just after the quench. Our measurements were found to be insensitive to variations in the gradient strength, duration, and orientation used during the initial-state preparation, and also to the delay (varied between 0 and 110 ms) between this preparation and the initiation of the spin amplifier. Obtaining $N_{\pm} \leq 3 \times 10^2$ and assuming an incoherent admixture of Zeeman sublevels, the thermal contribution to $G(0)|_0$ is $2N_{\pm}/N_0 \leq 3 \times 10^{-4}$. We checked also for technical noise that would induce extrinsic Zeeman transitions during the experiment. For the experimental conditions used for the measurements reported here, we found that a condensate starting in the $|m_z = -1\rangle$ state remained so for evolution times up to 400 ms following the quench, confirming the absence of noise-induced spin flips. For comparison, we also performed tests of the spin-mixing amplifier under experimental conditions in which noise-induced flips were indeed observed. Under these noisier conditions, the increased spin fluctuations input to the spin-mixing amplifier indeed yielded stronger magnetization outputs at early times following the quench.

Altogether, these results suggest that the state-purified paramagnetic samples were prepared with a near-zero spin

temperature. Nevertheless, it remains uncertain whether the zero-temperature amplifier theory should remain accurate out to a gain in the magnetization variance as high as 30 dB in a nonzero-temperature gas subject to constant heating and evaporation from the finite-depth optical trap. Indeed, previous work showed a strong influence of the noncondensed gas on spin dynamics in a two-component gaseous mixture [28]. We examined the role of thermal effects by comparing the amplification of magnetization at kinetic temperatures of 50 and 85 nK, obtained for different optical trap depths. We observed no variation, but note that the condensate fraction was not substantially varied in this comparison.

As indicated by the experimental uncertainties presented in Fig. 4, the comparison between a quantum amplification theory and experimental observations could be further constrained by an independent measure of the amplifier gain. The theoretical value for the amplifier gain is uncertain as a result of the uncertainty in Δa . In a future study, one could empirically determine the gain of the amplifier by studying the amplification of a coherent seed at a given k , e.g., a finite- k spin modulation produced by Raman scattering or a $k=0$ seed produced by tipping the condensate spinor before the quench to $0 < q < q_0$.

In conclusion, we have demonstrated the use of the spinor condensate as an amplifier of magnetization. Two tests of the amplifier have been performed simultaneously. First, assuming the input to the amplifier to have a white spatial spectrum and an initial variance consistent with quantum noise, we measure the tunable spatial spectrum and gain of the amplifier and find good agreement with predictions of a quantum linear-amplification theory. Second, assuming the amplifier to be described well by our theory, we find the magnitude and spatial distribution of magnetization fluctuations in the initial paramagnetic sample to be consistent with quantum noise. This demonstration of a low-noise spin amplifier holds promise for a host of applications and for future studies of quantum magnetism.

Moreover, by performing rapid quenches of paramagnetic condensates to variable q_f , we characterize the variation in the spin-mixing instability spectrum as one approaches the critical value of the quadratic shift, q_0 , from below. As discussed in several theoretical works, the nature of this variation determines the dynamical scaling behavior expected for variable-rate quenches across a phase transition between paramagnetic and ferromagnetic states [12,13,16,17]. The observation that paramagnetic gases are prepared with nearly quantum-limited spin fluctuations supports the possibility of quantitative investigations of quantum phase transitions with spinor gases.

We acknowledge insightful discussions with J. Moore and S. Mukerjee and experimental assistance from C. Smallwood. This work was supported by the NSF, the David and Lucile Packard Foundation, and the OLE Program of DARPA. Partial personnel and equipment support was provided by the LDRD Program of LBNL under Department of Energy Contract No. DE-AC02-05CH11231. S.R.L. acknowledges support from the NSERC.

- [1] T.-L. Ho, Phys. Rev. Lett. **81**, 742 (1998).
- [2] T. Ohmi and K. Machida, J. Phys. Soc. Jpn. **67**, 1822 (1998).
- [3] J. Stenger, S. Inouye, D. M. Stamper-Kurn, H.-J. Miesner, A. P. Chikkatur, and W. Ketterle, Nature (London) **396**, 345 (1998).
- [4] H. Schmaljohann, M. Erhard, J. Kronjager, M. Kottke, S. van Staa, L. Cacciapuoti, J. J. Arlt, K. Bongs, and K. Sengstock, Phys. Rev. Lett. **92**, 040402 (2004).
- [5] M. S. Chang, C. D. Hamley, M. D. Barrett, J. A. Sauer, K. M. Fortier, W. Zhang, L. You, and M. S. Chapman, Phys. Rev. Lett. **92**, 140403 (2004).
- [6] H. J. Miesner, D. M. Stamper-Kurn, J. Stenger, S. Inouye, A. P. Chikkatur, and W. Ketterle, Phys. Rev. Lett. **82**, 2228 (1999).
- [7] M.-S. Chang, Q. Qin, W. X. Zhang, L. You, and M. S. Chapman, Nat. Phys. **1**, 111 (2005).
- [8] L. Sadler, J. M. Higbie, S. R. Leslie, M. Vengalattore, and D. M. Stamper-Kurn, Nature (London) **443**, 312 (2006).
- [9] M. Vengalattore, S. R. Leslie, J. Guzman, and D. M. Stamper-Kurn, Phys. Rev. Lett. **100**, 170403 (2008).
- [10] M. Vengalattore, J. M. Higbie, S. R. Leslie, J. Guzman, L. E. Sadler, and D. M. Stamper-Kurn, Phys. Rev. Lett. **98**, 200801 (2007).
- [11] W. Zhang, D. L. Zhou, M. S. Chang, M. S. Chapman, and L. You, Phys. Rev. Lett. **95**, 180403 (2005).
- [12] A. Lamacraft, Phys. Rev. Lett. **98**, 160404 (2007).
- [13] H. Saito, Y. Kawaguchi, and M. Ueda, Phys. Rev. A **75**, 013621 (2007).
- [14] R. Movshovich, B. Yurke, P. G. Kaminsky, A. D. Smith, A. H. Silver, R. W. Simon, and M. V. Schneider, Phys. Rev. Lett. **65**, 1419 (1990).
- [15] M. Mück, J. B. Kycia, and J. Clarke, Appl. Phys. Lett. **78**, 967 (2001).
- [16] B. Damski and W. H. Zurek, Phys. Rev. Lett. **99**, 130402 (2007).
- [17] M. Uhlmann, R. Schutzhold, and U. R. Fischer, Phys. Rev. Lett. **99**, 120407 (2007).
- [18] H. Saito and M. Ueda, Phys. Rev. A **72**, 023610 (2005).
- [19] G. I. Mias, N. R. Cooper, and S. M. Girvin, Phys. Rev. A **77**, 023616 (2008).
- [20] E. G. M. van Kempen, S. J. J. M. F. Kokkelmans, D. J. Heinzen, and B. J. Verhaar, Phys. Rev. Lett. **88**, 093201 (2002).
- [21] F. Gerbier, A. Widera, S. Fölling, O. Mandel, and I. Bloch, Phys. Rev. A **73**, 041602(R) (2006).
- [22] By comparing experiments with similar q_f but variable q_μ , the admixing of hyperfine levels produced by the applied microwave field was found not to influence the dynamics of the $F=1$ gas.
- [23] We measure also the longitudinal magnetization of the condensate, but find that it remains small (<15% of the maximum magnetization).
- [24] A. Widera, F. Gerbier, S. Fölling, T. Gericke, O. Mandel, and I. Bloch, New J. Phys. **8**, 152 (2006).
- [25] I. Carusotto and E. J. Mueller, J. Phys. B **37**, S115 (2004).
- [26] J. D. Sau *et al.*, e-print arXiv:0904.1199.
- [27] M. Baraban, H. F. Song, S. M. Girvin, and L. I. Glazman, Phys. Rev. A **78**, 033609 (2008).
- [28] J. M. McGuirk, D. M. Harber, H. J. Lewandowski, and E. A. Cornell, Phys. Rev. Lett. **91**, 150402 (2003).